Liquid Crystals
Publication details, including instructions for authors and subscription information:
http://www.informaworld.com/smpp/title~content=t713926090

Conformational analysis of 1,2-dimethoxyethane and 1,2-diphenyloxyethane incorporated in nematic liquid crystals

Akihiro Abe[a]; Emi Iizumi[a]; Noritaka Kimura[a]
[a] Department of Polymer Chemistry, Tokyo Institute of Technology, Tokyo, Japan

To cite this Article Abe, Akihiro , Iizumi, Emi and Kimura, Noritaka(1994) 'Conformational analysis of 1,2-dimethoxyethane and 1,2-diphenyloxyethane incorporated in nematic liquid crystals', Liquid Crystals, 16: 4, 655 — 670
To link to this Article: DOI: 10.1080/02678299408036537
URL: http://dx.doi.org/10.1080/02678299408036537

LIQUID CRYSTALS, 1994, VOL. 16, NO. 4, 655–670

Conformational analysis of 1,2-dimethoxyethane and 1,2-diphenyloxyethane incorporated in nematic liquid crystals

by AKIHIRO ABE*, EMI IIZUMI and NORITAKA KIMURA
Department of Polymer Chemistry, Tokyo Institute of Technology, Ookayama, Meguro-ku, Tokyo 152, Japan

(*Received 28 July 1993; accepted 24 September 1993*)

The conformations of flexible chain molecules incorporated in a nematic environment have been investigated. The phase behaviours and orientational characteristics of 1,2-dimethoxyethane (DME) dissolved in 4′-methoxybenzylidene-4-*n*-butylaniline at low solute mol fraction have been reported in our previous paper. In this work, proton–proton and carbon–carbon dipolar coupling constant measurements were attempted in addition to ^{2}H NMR observations of quadrupolar splittings. These conformation-dependent properties were analysed according to the rotational isometric state (RIS) simulation scheme previously proposed. Our treatment rests on the assumption that the molecular axis of the chain should tend to align along the nematic field. Studies were further extended to a mixture of 1,2-diphenyloxyethane (DPE) with a nematic liquid crystal, 4,4′-azoxyanisole. Replacement of the terminal methyl groups in DME by phenyl groups leads to DPE. The results of the analysis indicate that the fraction of elongated conformers such as *ttt* tends to increase significantly on going from the isotropic to the liquid crystalline solution: DME; 9·4 to 15·6 per cent and DPE; 12·3 to 20·0 per cent. The *tgt* form (tg^+t or tg^-t) is the lowest-energy arrangement of these molecules. The fraction of this conformer also increases in DPE (26·8 to 40·0 per cent), while it decreases in DME (25·7 to 18·8 per cent). The conformational distributions of chain molecules were found to remain invariant over the range of concentration (0·5–6·0 mol per cent) and temperature (22·0–44·5°C) studied. It has been concluded that the observed variation of proton dipolar and deuterium quadrupolar couplings with concentration and temperature mainly arises from the orientational order of the molecular axis, which varies sensitively with the alignment of the surrounding solvent molecules. These results suggest that flexible chains are also participating in the nematic interaction by adjusting their configurations so as to enhance favourable interactions and suppress unfavourable steric repulsions when accommodated in an anisotropic potential field.

1. Introduction

In our previous studies [1], equilibrium phase transitions in binary mixtures comprising chain molecule/liquid crystalline solvent have been examined. Flexible chains such as 1,2-dimethoxyethane (DME) and its higher homologues $CH_3O(CH_2CH_2O)_nCH_3$ ($n=1$ to 3) were found to be more disruptive of the nematic order of surrounding mesomorphic molecules such as 4′-methoxybenzylidene-4-*n*-butylaniline (MBBA), than the corresponding hydrocarbon analogues. In an attempt to elucidate molecular structure–phase stability relations, the ^{2}H NMR technique has been extensively employed. Deuterium quadrupolar splitting data ($\Delta\nu$) provide

* Author for correspondence.

0267–8292/94 $10·00

information regarding the orientational order of solute chain molecules, as well as those of the nematic solvent MBBA. The values of $\Delta\nu$ due to the methylene or methyl deuterons of the solute fall on a single curve when plotted against the order parameter of the host MBBA. These observations strongly suggest that flexible chains are also participating in the nematic interaction. In all the systems examined, including *n*-hexane/MBBA, the ratio of the quadrupolar splittings $\Delta\nu_i/\Delta\nu_j$, which represents the relative orientation of the CD bonds at sites *i* and *j*, were found to remain nearly invariant over a wide range of concentration and temperature. It has been concluded from the rotational isomeric state (RIS) analysis that the flexible chain molecules examined prefer to assume somewhat more elongated forms in order to facilitate alignment in the nematic field relative to those assumed in a conventional isotropic solution. The amount of information obtained through ^{2}H NMR measurements was however found to be insufficient for a reliable estimate of conformer fractions. In the previous work [1], we analysed the proton dipolar and deuterium quadrupolar coupling data of Gochin *et al.*, for the *n*-hexane/EK11650 (Kodak) system [2], and the conformer fractions were compared with those reported by the original authors, as well as by Samulski *et al.* [3]. Through these analyses, the importance of dipolar coupling data was recognized. In this work, proton–proton and carbon–carbon dipolar coupling measurements were therefore attempted in addition to the ^{2}H NMR observations.

Studies were further extended to mixtures of 1,2-diphenyloxyethane (DPE) $\phi OCH_2CH_2O\phi$ with nematic liquid crystals. Replacement of the terminal methyls by phenyl groups in DME leads to DPE. When compared in their extended conformations, the anisotropy of the chain is higher in the latter compound. According to Martire *et al.* [4], the slopes of the nematic–isotropic phase boundary lines at low mol fractions provide a measure of the compatibility of non-mesomorphic solutes with the nematic phase. The phase stabilities thus estimated are nearly equivalent for the two binary mixtures DME/MBBA and DPE/MBBA, indicating that the effect on the nematic order is also similar [5]. To facilitate proton–proton dipolar coupling measurements on DPE, use of a perdeuteriated solvent was required. For this reason, 4,4′-azoxyanisole (PAA) was employed as a nematic solvent for DPE. Reagent grade perdeuteriated PAA is commercially available. The results of the RIS analysis are therefore reported for a binary mixture comprising DPE/PAA.

After completion of this work, we learned that Cheung and Emsley [6] had carried out ^{2}H NMR measurements on DPE in liquid crystal hosts such as Phase 5 (E. Merck), EBBA (Kodak), and ZLI 1132 (E. Merck), and examined the results according to their theoretical model. In this study, the torsional energy intrinsic to the central C–C bond was estimated by the analysis of the ^{13}CH satellite side band spectrum observed in acetone as solvent. The conformational distributions derived for both the isotropic and anisotropic media are somewhat inconsistent with our results. The cause of the discrepancy will be discussed in the last section.

2. Experimental

2.1. *Chemicals*

Reagent grade samples of MBBA, DME, and DPE are commercially available. A perdeuteriated sample of PAA was purchased from Aldrich. The degree of deuteriation was certified to be 96 per cent. The other isotope-labelled compounds used were prepared as described below.

2.2. *Dimethoxyethane-d_6(DME-d_6)* $CD_3OCH_2CH_2OCD_3$

The compound was synthesized from ethyleneglycol and methyl iodide-d_3 according to the procedure described by Capinjola [7]. The fraction distilling at 80–88°C was collected.

2.3. *DME-$^{13}C_2$* $CH_3O^{13}CH_2{}^{13}CH_2OCH_3$

Ethyleneglycol-$^{13}C_2$ is commercially available. The preparative procedure for the dimethyl ether is the same as that given above.

2.4. *Diphenoxyethane-d_{10}(DPE-d_{10})* $C_6H_2D_3OCD_2CD_2OC_6H_2D_3$

2,4,6-Deuteriated phenol was prepared by following the method of Zimmermann [8]. The alkylation reaction with 1,2-dibromoethane-d_4 (commercial) has been described by Cope [9]. The sample was purified by repeated recrystallization (m.p. 96°C).

2.5. *DPE-ϕ-d_{10}* $C_6D_5OCH_2CH_2OC_6D_5$

Perdeuteriated phenol was purchased commercially. The reaction with 1,2-dibromoethane was performed as described above.

2.6. *4,4'-Azoxyanisole-d_4 (PAA-d_4)* $CH_3OC_6H_2D_2N{=}NC_6H_2D_2OCH_3$

PAA-d_4 was prepared from 2,6-deuteriated nitrosophenol according to the procedure given in [10]. Deuteriation at 2,6-positions facilitates estimation of the orientational order parameter of the nematic solvent in the DPE/PAA mixture by the ^{2}H NMR method.

2.7. *Measurements*

The ^{1}H–{^{2}H} decoupled NMR spectra were recorded at 250·13 and 500·14 MHz, respectively, using Bruker AC-250 and AMX-500 spectrometers. ^{2}H decoupling was achieved with GARP modulation [11]. The decoupler was on for the duration of the acquisition time (0·5 s), and a 2 s delay was used between pulses so as to allow the sample to remain at ambient temperatures. The FT spectra contain 16 K data points for the 16 kHz spectral width.

^{2}H NMR measurements were performed using a JEOL JNM-GSX-500 spectrometer operating at 76·78 MHz. The FT spectra contain 16 K data points for the 40 kHz spectral width. ^{13}C–{^{1}H} decoupled NMR spectra were recorded on the same apparatus operating at 125·78 MHz. The FT spectra contain 32 K data points for the 30 kHz spectral width. All measurements were carried out in the non-spinning mode.

3. Experimental results

^{1}H NMR studies were performed for $CD_3OCH_2CH_2OCD_3$ (DME-d_6) dissolved in nematic MBBA. Given in figure 1 is the spectrum observed for the deuterons on the terminal methyl groups. The convolution difference technique was employed to reduce the very broad background of MBBA. For $C_6D_5OCH_2CH_2OC_6D_5$ (DPE-ϕ-d_{10}), a similar technique was found to be ineffective because of the line broadening due to insufficient motional narrowing in the highly aromatic medium. To avoid this problem, measurements were carried out using a 96 per cent deuteriated sample of PAA. An example of the spectra obtained is shown in figure 2. In the anisotropic liquid crystalline environment, the individual methylene hydrogens are non-equivalent. The spectrum was analysed by assuming an AA'A''A''' spin system according to the scheme

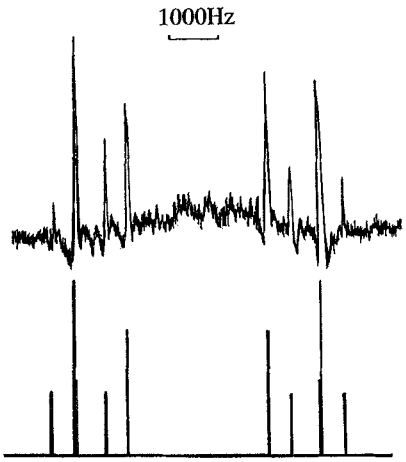

Figure 1. An example of ^{1}H NMR spectra obtained for DME-d_6 in nematic MBBA (6 mol %, 7°C), the terminal methyl deuterons being irradiated. The dipolar coupling constants D_{CH_2} and D_{CH-CH} (D_{13}, D_{14}) were obtained by assuming an AA'A"A''' spin system: $-O-CH_1H_2-CH_3H_4-O-$. Shown for comparison is the calculated stick spectrum.

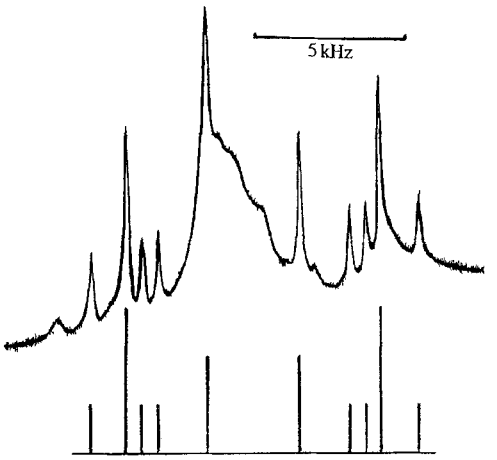

Figure 2. An example of ^{1}H NMR spectra observed for DPE-ϕ-d_{10} in nematic PAA (2·0 mol %, 121·7°C), the terminal phenyl deuterons being irradiated. The spin analysis was carried out by assuming an AA'A'A''' system. The calculated results are shown by the stick spectrum.

proposed by Englert *et al.* [12, 13]. The results of simulations are illustrated by the stick spectra in figures 1 and 2, respectively, for DME and DPE.

Figure 3 indicates the ^{13}C NMR spectrum obtained for DME-$^{13}C_2$ dissolved in MBBA (6 mol per cent). The carbon–carbon dipolar coupling constant D_{CC} can be determined from the separation of the intense doublet characteristic of the methylene carbon [13]. Examples of the ^{2}H NMR spectra have been reported in our previous paper [1] and are thus omitted here.

DME/MBBA: ^{2}H NMR measurements were carried out for DME-d_{10} involved in MBBA. Values of the two $\Delta\nu$s, one for the methylene and the other for the methyl

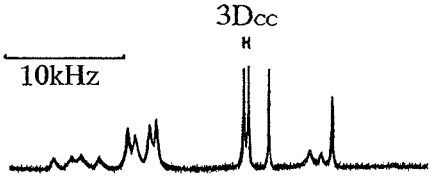

Figure 3. An example of ^{13}C NMR spectra of DME-$^{13}C_2$ dissolved in nematic MBBA (6·0 mol%, 30°C). The splitting corresponding to $3D_{CC}$ is indicated in the diagram [13].

Table 1. ^2H NMR data for DME-d_{10} observed in nematic MBBA.

Concentration/mol per cent	Temperature/°C	$\Delta\nu_{CD_2}$/Hz	$\Delta\nu_{CD_3}$/Hz	D_{CD_2}/Hz	D_{CD_3}/Hz
0·5	44·5	−8060	−2965	16·5	8·8
	44·0	−8701	−3202	16·3	9·3
	42·0	−10679	−3959	22·0	11·8
	40·0	−11504	−4279	22·3	12·3
	37·0	−12876	−4827	27·8	15·8
	27·5	−15264	−5832	32·0	18·8
	22·0	−16400	−6340	35·3	20·8
2·0	27·5	−14531	−5551	30·8	18·0
4·0	27·5	−13206	−5039	28·3	16·0
6·0	27·5	−11764	−4485	24·0	13·8

deuterons, and dipolar couplings D_{CD_2} and D_{CD_3} observed concomitantly are assembled in table 1. These results indicate that the sign of $\Delta\nu_{CD_2}$ is negative and that of D_{CD_2} is positive [14]. (The opposite assignment of the sign is inconsistent with the molecular orientation in the nematic field.) Adoption of the negative sign for $\Delta\nu_{CD_3}$ is tentative at this stage. The RIS analysis described in a later section will provide proof for this assignment (see table 7). The values of the proton dipolar couplings D_{CH_2} (geminal) and D_{CH-CH} (vicinal) derived at solute mol fractions of 2·0, 4·0, and 6·0 per cent are listed in table 2. From the relation

$$D_{CH_2} = \left(\frac{\gamma_H^2}{\gamma_D^2}\right) D_{CD_2} \tag{1}$$

$D_{CH_2} > 0$ and thus D_{CH-CH} $(D_{13}, D_{14}) < 0$. Since the proton dipolar and deuterium quadrupolar coupling measurements were carried out separately by using different apparatus, precise matching of the sample temperature was difficult. To circumvent such difficulties, the deuterium quadrupolar splittings $\Delta\nu$ due to the deuterons situated on the terminal groups were simultaneously observed, and calibration curves were constructed by plotting D_{CH_2} and D_{CH-CH} against $\Delta\nu_{CD_3}$ thus determined.

The values of D_{CC} observed under various conditions are listed in table 3. Some of the experiments were carried out for mixtures with DME-d_6. The D_{CC} versus $\Delta\nu_{CD_3}$ plot was then used for the calibration of temperatures.

DPE/PAA: Deuterium quadrupolar and proton dipolar coupling constants obtained for DPE dissolved in a nematic solvent PAA are summarized in tables 4 and 5, respectively. In table 5, temperatures were calibrated by using the deuterium quadrupolar splitting data observed simultaneously for the solvent molecule PAA. In the ^2H NMR spectra obtained for DPE-d_{10}, the splittings due to the *ortho*-proton of

Table 2. Proton–proton dipolar couplings of DME-d_6 observed in nematic MBBA.

Concentration/mol per cent	Temperature/°C	D_{CH_2}/Hz	D_{CH-CH}/Hz	
2·0	34·6	1016	−221	−85
	28·3	1220	−280	−108
4·0	31·2	959	−208	−88
	26·4	1114	−248	−97
	22·4	1252	−292	−116
	18·7	1356	−313	−132
6·0	31·7	775	−173	−69
	29·9	861	−195	−77
	24·6	1083	−245	−100
	22·5	1160	−265	−105
	19·1	1279	−312	−124
	12·9	1470	−360	−151

Table 3. Carbon–carbon dipolar couplings of DME-$^{13}C_2$ observed in nematic MBBA.

Concentration/mol per cent	Temperature/°C	D_{CC}/Hz
0·5	43·0	−120
	41·0	−129
	38·0	−153
	33·5	−172
	27·0	−197
2·0	40·0	−121
	37·0	−141
	32·5	−158
	27·5	−179
	22·0	−191
4·0	36·0	−117
	34·0	−127
	30·0	−149
	25·0	−170
	22·0	−179
6·0	32·0	−97
	30·0	−121
	27·0	−137
	23·0	−158
	20·0	−170

Table 4. ^{2}H NMR data for DPE-d_{10} observed in nematic PAA, and the order parameters of the *para*-axis of the terminal phenyl groups estimated therefrom.

Concentration/mol per cent	Temperature/°C	$\Delta\nu_{CD_2}$/Hz	$\Delta\nu_p$/Hz	$\lvert\Delta\nu_0\rvert$†/Hz	D_{HD}‡/Hz	S^R_{ZZ}	$S^R_{XX}-S^R_{YY}$§
0·5	132	−18522	47913	453	−226	0·182	0·048 ± 0·004
	130	−20363	53421	416	−222	0·179	0·047 ± 0·003
	128	−22494	58229	244	−255	0·206	0·055 ± 0·003
	125	−24867	64657	0	−276	0·223	0·059
	122	−26841	69378	192	−300	0·242	0·065 ± 0·003
	118	−28857	75574	614	−307	0·248	0·066 ± 0·004
2·0	128	−19384	50940	406	−203	0·164	0·044 ± 0·004
	127	−20496	53573	325	−226	0·182	0·048 ± 0·003
	125	−22603	59401	126	−250	0·202	0·054 ± 0·002
	123	−24050	63201	0	−271	0·219	0·058
	120	−26506	69462	199	−300	0·242	0·064 ± 0·002
	117	−27771	72352	379	−298	0·241	0·064 ± 0·004

† The signs of the deuterium quadrupolar coupling constant at the *ortho*-position are not definite.

‡ The experimental error involved in these measurements amounts to 10–20 Hz.

§ Probable ranges for both possible signs of $\Delta\nu_0$ are indicated as uncertainties. In these calculations, the angle $\angle C^{ph}C^{ph}H(D)$ was assumed to be 120·0°.

Table 5. Proton–proton dipolar couplings of DPE-ϕ-d_{10} observed in nematic perdeuteriated PAA.

Concentration/mol per cent	Temperature/°C	D_{CH_2}/Hz	D_{CH-CH}/Hz	
2·0	124·9	1969	−633	−477
	121·7	2278	−736	−556
	118·8	2507	−812	−618

the terminal phenyl group were found to be very small and the sign of the observed $\Delta\nu_0$ values could not be determined. In this system, dipolar splitting D_{HD} arising from the coupling between the *o*-deuteron and the neighbouring *m*-hydrogen was used, as a supplement to the quadrupolar splitting $\Delta\nu_p$, to determine the orientational ordering (S^R_{ZZ}) of the *para*-axis of the phenyl group. The biaxiality term $S^R_{XX}-S^R_{YY}$ varies slightly depending on the sign of $\Delta\nu_0$: probable ranges for both possible signs are appended to each estimate in table 4.

4. RIS analysis

The structural data for DME and DPE adopted in the present analysis are summarized in table 6 [15]. The angle ∠DCD was assumed to be 107·9° as suggested from the electron diffraction studies on propane [16]. Rotational states adopted are as follows: DME; 0°, ±100° (C–O) and 0°, ±120° (C–C), and DPE; 0°, ±100° (C–O) and 0°, ±120° (C–C). A schematic representation of the DME molecular system and definition of the molecular axis are illustrated in figure 4. The value of the dipolar coupling D_{lm} between atoms l and m can be conventionally expressed as

$$D_{lm}=-\frac{h\gamma_l\gamma_m}{4\pi^2}\left\{\left\langle S_{ZZ}\frac{3\cos^2\theta_{lmZ}-1}{2r_{lm}^3}\right\rangle+\left\langle (S_{XX}-S_{YY})\frac{\cos^2\theta_{lmZ}-\cos^2\theta_{lmY}}{2r_{lm}^3}\right\rangle\right\} \quad (2)$$

where h is the Planck constant, γ_l and γ_m denote the gyromagnetic ratio, r_{lm} is the atomic distance between *l* and *m*, *X*, *Y*, and *Z* are the principal axes of the orientational order matrix, ϕ_{lma} (a denotes *X*, *Y*, or *Z*) is the angle between the vector connecting l and m and axis a, S_{aa} is the diagonal element of the orientational order matrix defined with respect to the nematic director, and the $\langle\ \rangle$ designate statistical mechanical averages over all allowed conformations. The observed deuterium quadrupolar splitting $\Delta\nu_i$ is given as follows:

$$\Delta\nu_i=\frac{3}{2}\frac{e^2qQ}{h}\left\{\left\langle S_{ZZ}\frac{3\cos^2\theta_{iZ}-1}{2}\right\rangle+\left\langle (S_{XX}-S_{YY})\frac{\cos^2\theta_{iX}-\cos^2\theta_{iY}}{2}\right\rangle\right\} \quad (3)$$

where e^2qQ/h is the quadrupolar coupling constant, and θ_{ia} is the angle defined by the *i*th C–D bond and axis a. The coupling constants were taken to be 174 [17] and 181 [18] kHz, respectively, for aliphatic and aromatic CD bonds. We adopt a single-ordering-matrix scheme [19] in which the orientational order parameters S are taken to be identical for all the conformers involved in the liquid crystalline phase. In this treatment, the molecular axis was defined for each conformer in the direction along the principal axis of inertia with the minimum moment [2, 20]. In the calculation, the methyl, methyleme, and phenyl groups were treated as united atoms. The masses of atoms and groups were assumed to reside at the centres. Following the previous

Table 6. Geometrical parameters adopted for DME and DPE.

Bond	Length/Å	Bond angle	Angle/degree
C–H	1·10	∠HCO (CH_3)	111·0
C–C	1·53	∠HCO (CH_2)	109·3
C–O	1·43	∠COC	111·5
C^{ph}–O	1·36	∠CCO	111·5
C^{ph}–C^{ph}	1·40	∠C^{ph}OC	120·0

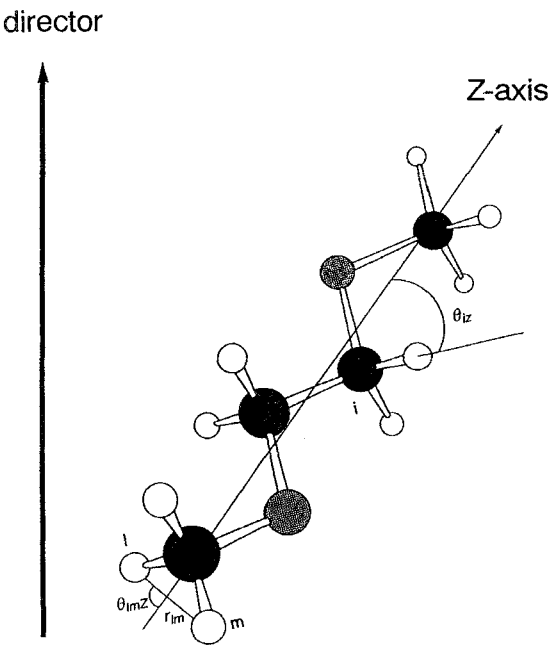

Figure 4. An illustration of angles required for the definition of proton dipolar and deuterium quadrupolar couplings with respect to the long molecular axis. Depicted in the figure is DME in its all *trans*-conformation.

treatment [21], we adopt a scheme in which the relative importance of a given conformer can be expressed as a product of statistical weight factors assigned to the constituent bonds. In the iterative calculations, statistical weight parameters ρ and σ were assigned respectively to the *gauche* state of C–O and C–C bonds (cf. figure 5). On the expectation that the second-order interaction such as $g^{\pm}g^{\mp}$ should be of rare occurrence in the nematic environment, the weight was set equal to zero (cf. figure 5). The validity of this assumption will be examined later. The simulation was carried out according to the simplex method [22], and the order parameters of the molecular axes S_{ZZ} and S_{XX}–S_{YY} were adjusted so as to minimize the reliability factor

$$R(\text{per cent}) = \sqrt{\left[\frac{\Sigma(A_{\text{calc'd}} - A_{\text{obs'd}})^2}{\Sigma A_{\text{obs'd}}^2}\right]} \times 100. \tag{4}$$

The experimental data collected in table 7 are those obtained for DME/MBBA at 6·0 solute mol% and 27·5°C. The analysis indicates that the contribution from the

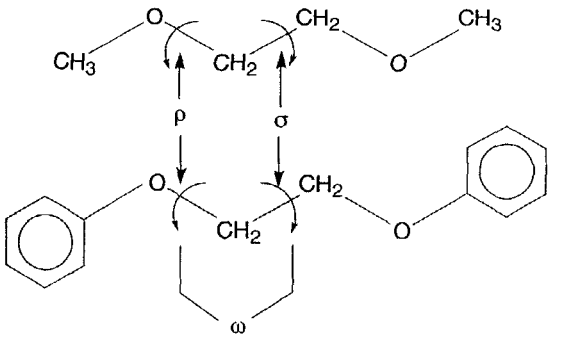

Figure 5. Definition of statistical weight factors for the first and second order *gauche* interactions. Weights are expressed relative to the *trans*-state.

Table 7. Comparison of observed and calculated coupling constants of DME involved in nematic MBBA.

	Observed/Hz†	Calculated/Hz
$\Delta\nu_{CD_3}$	−4485	−4485
$\Delta\nu_{CD_2}$	−11764	−11764
D_{CD_3}	13·8	14·1
D_{CD_2}	24·0	24·1
D_{CH-CH}	−229	−196
	−91	−90
D_{CH_2}	1018	989
D_{CC}	−138	−152

† 6·0 solute mol% at 25°C.

biaxiality term in equations (2) and (3) is relatively small within the range $S_{XX}-S_{YY}=0$ to 0·05. Shown in the last column of table 7 are the results of simulation obtained at $S_{XX}-S_{YY}=0{\cdot}025$. The observed coupling constants are reasonably well reproduced. The conformer fractions estimated therefrom are summarized in table 8, where the order parameters of the molecular axis derived simultaneously are given in the footnote. The conformer fractions calculated for the isotropic state [23] are listed in the last column. Comparison indicates that fractions for *ttt* and $ttg^{\pm}$ increase significantly at the expense of $tg^{\pm}t$. Inclusion of a parameter designating the four-bond interaction such as $g^{\pm}g^{\mp}$ enhanced the *R*-factor in the simulation, but conformer fractions were found to be practically unaffected.

A similar analysis has been carried out for the DPE/PAA system. The experimental data listed in table 9 are those obtained at 2·0 solute mol per cent and 123°C. The carbon–carbon dipolar coupling D_{CC} could not be measured in this system. Simulations were performed according to the scheme defined by equations (2)–(4). Contribution from the biaxiality term was found to be relatively unimportant in the range $S_{XX}-S_{YY}=0$ to 0·05. In table 9, the results obtained for $S_{XX}-S_{YY}=0{\cdot}025$ are compared with those observed. Here the agreement for $\Delta\nu_p$ tends to be improved when smaller values of $S_{XX}-S_{YY}$ are assumed. Since an accurate estimation of the biaxiality term is beyond the scope of the present study, comparison for $\Delta\nu_0$ is not included. The conformer fractions thus derived are listed in table 10, where the isotropic fractions estimated from the vicinal coupling constant measurements in benzene are also

Table 8. Conformer probabilities of DME in nematic MBBA, compared with those in the isotropic state.

Conformation† (multiplicity)		in MBBA‡	Free state§
ttt	(1)	15·6	9·4
$tg^{\pm}t$	(2)	18·8	25·7
$ttg^{\pm}$	(4)	4·4	1·8
$tg^{\pm}g^{\pm}$	(4)	5·3	4·8
$g^{\pm}tg^{\pm}$	(2)	1·2	0·3
$g^{\pm}tg^{\mp}$	(2)	1·2	0·3
$g^{\pm}g^{\pm}g^{\pm}$	(2)	1·5	0·9

† For example, the notation $tg^{\pm}t$ represents the individual isomer $tg^{+}t$ or $tg^{-}t$. Similarly $tg^{\pm}g^{\pm}$ should be read as $tg^{+}g^{+}$ or $tg^{-}g^{-}$.

‡ The order parameters of the molecular axis obtained concomitantly are $S_{ZZ}=0{\cdot}115$ and $S_{XX}-S_{YY}=0{\cdot}025$.

§ Conformational statistical weight parameters required for the calculation were taken from [23]: $E_{\rho}=4{\cdot}2$, $E_{\sigma}=-2{\cdot}5$, and $E_{\omega}=2{\cdot}2$, the units being kJ mol^{-1}. The remaining fractions are $tg^{\pm}g^{\mp}(4)=2{\cdot}0$, $g^{\pm}g^{\pm}g^{\mp}(4)=0{\cdot}4$, and $g^{\pm}g^{\mp}g^{\pm}(2)=0{\cdot}1$.

Table 9. Comparison of observed and calculated coupling constants of DPE involved in nematic PAA.

	Observed/Hz†	Calculated/Hz
$\Delta\nu_{CD_2}$	−24050	−24056
$\Delta\nu_{p}$	63201	58521
D_{HD}	−271	−267
D_{CH-CH}	−780	−791
	−592	−628
D_{CH_2}	2410	2355

† 2·0 solute mol% at 123°C.

Table 10. Conformer probabilities of DPE in nematic PAA, compared with those in the isotropic state.

Conformation† (multiplicity)		in PAA‡	Free state§
ttt	(1)	20·0	12·3
$tg^{\pm}t$	(2)	40·0	26·8
$ttg^{\pm}$	(4)	0·0	2·4
$tg^{\pm}g^{\pm}$	(4)	0·0	5·2

† See the footnote to table 8.

‡ The order parameters of the molecular axis obtained concomitantly are $S_{ZZ}=0{\cdot}232$ and $S_{XX}-S_{YY}=0{\cdot}025$.

§ Statistical weight parameters used in the calculation are given in the Appendix. The remaining fractions are $g^{\pm}tg^{\pm}(2)=0{\cdot}4$, $g^{\pm}tg^{\mp}(2)=0{\cdot}4$, and $g^{\pm}g^{\pm}g^{\pm}(2)=1{\cdot}0$.

included for comparison. (The results of ^1H and ^{13}C NMR measurements on DPE, and the elucidation of conformational energy parameters by the RIS method are described in the Appendix). In contrast to the DME/MBBA mixture, fractions of *ttt* and $tg^{\pm}t$ are both enhanced, while those of $ttg^{\pm}$ and $tg^{\pm}g^{\pm}$ tend to be entirely suppressed. As an inspection of a proper molecular model should reveal, a rectilinear alignment of the phenyl groups located on both terminals is guaranteed in the former conformers. Since these terminal phenyl groups are mutually disoriented in the latter arrangements, their inclusion may cause an appreciable disturbance in the nematic alignment of the surrounding molecules.

5. Discussion

In the previous treatment of DME and its homologues, the deuterium quadrupolar splitting ratios $\Delta\nu_i/\Delta\nu_j$, which are in principle only sensitive to the conformation of the flexible solute, have been found to remain invariant over a wide range of concentration and temperature [1]. An essentially identical behaviour has been observed for the DPE/PAA mixture when $\Delta\nu_i/\Delta\nu_j$ ratios are plotted against concentration and temperature. These results indicate that the observed concentration and temperature dependences are mainly due to variation of the order parameter of the molecular axis S_{ZZ}, the conformer fraction being nearly unaffected. The values of S_{ZZ} obtained from the RIS simulation are plotted as a function of temperature in figures 6 and 7. As previously noted by Luckhurst *et al.* [24], and Kronberg *et al.* [25], the S_{ZZ} versus temperature curves shown in these figures are superimposable when plotted against the temperature ratio T/T_{NI}. The orientational order of the solute should vary sensitively with the alignment of the nematic solvent. Shown in the insets of figures 6 and 7 are the plots of S_{ZZ} against the order parameter of surrounding solvent molecules S^{M}_{ZZ}, which has been determined according to the procedure given in our previous work [1]. These results suggest that flexible chains are also participating in the nematic interaction.

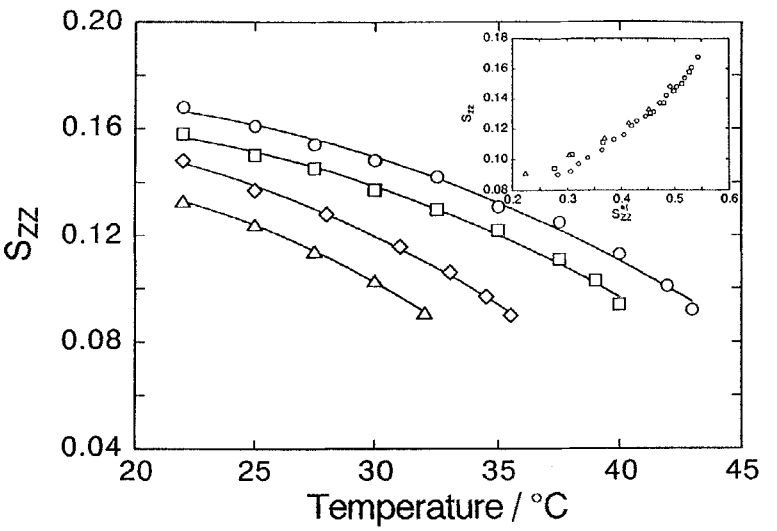

Figure 6. Variation of the orientational order parameter S_{ZZ} (DME) as a function of temperature. Shown in the inset are the plots of S_{ZZ} versus S^{M}_{ZZ} of the coexisting nematic solvent (MBBA). Values of S^{M}_{ZZ} were taken from our previous work [1]. ○, 0·5; □, 2·0; ◇, 4·0; △, 6·0 mol%.

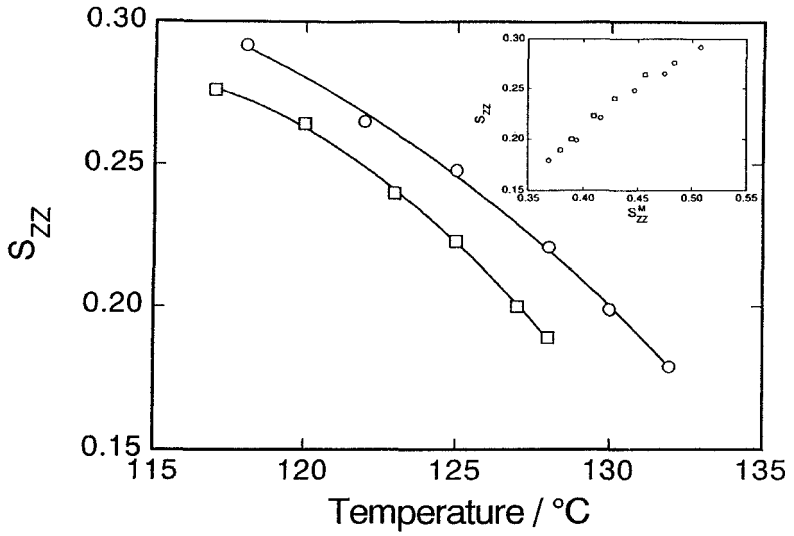

Figure 7. Variation of the order parameter S_{ZZ} (DPE) as a function of temperature. Shown in the inset are the plots of S_{ZZ} versus S^M_{ZZ} of the coexisting nematic solvent (PAA). ○, 0·5; □, 2·0 mol %.

Since the dipole moment of both DME and DPE is only moderate, the dispersion interaction through the anisotropy of polarizability may be the major cause of molecular ordering of these molecules in the nematic environment [26]. In summary, it should be pointed out that chain molecules may adjust configurations so as to enhance favourable interactions and suppress unfavourable steric repulsions when accommodated in an anisotropic potential field. By and large, conformational cooperativity may extend over a long-range when the chain molecule comprises more than several bonds.

The conformational distributions estimated for DPE in this work are quite different from those reported by Cheung *et al.* [6], for both isotropic and anisotropic states. In the following, we present our comments on the major cause of the discrepancy. (The symbols are adopted from their paper.)

(1) The steric interactions involving two consecutive bond rotations are entirely neglected in Cheung *et al*'s treatment. (This corresponds to an assumption that $\omega \approx 1$ in our scheme.) Such an assumption should lead to a somewhat unrealistic conformer distribution. For example, in table 2 of reference [6(*b*)], fractions of $tg^{\pm}g^{\pm}$ and $tg^{\pm}g^{\mp}$ are identical in the isotropic state ($P^{iso} = 0{\cdot}14$), and they are nearly equivalent even in the liquid crystalline state ($P^{LC} = 0{\cdot}12$ and 0·13, respectively). These situations are unlikely to occur.

(2) Cheung *et al.* have examined the ^{13}CH-satellite side band spectrum in acetone. In table 1 of [6(*a*)], the difference between the two vicinal proton couplings $L(=|J_{13}-J_{14}|)$ seems to be incorrectly printed. In combination with $N(=|J_{13}+J_{14}|)=9{\cdot}6$ Hz, we obtain $J_{13}=6{\cdot}4$ Hz and $J_{14}=3{\cdot}2$ Hz. (In our notation, $J_{13}={}^3J_{HH}$ and $J_{14}={}^3J'_{HH}$.) Similar coupling constants have been observed in C_6D_6 and DMSO-d_6 in our laboratory. The RIS analysis of these results is presented in the Appendix.

(3) Since the temperature dependence of L and N values has not been determined in Cheung *et al.*'s measurements, an unambiguous elucidation of the sign for L is impossible. Assuming that the thermal behaviour is similar to that observed in C_6D_6 or DMSO-d_6 (*cf.* Appendix), the temperature coefficient of L is negative. From the

fraction ($n_t = 0{\cdot}12$) given by Cheung *et al.*, one obtains $E_{tg} = -3{\cdot}24\,\mathrm{kJ\,mol^{-1}}$ in reasonable agreement with our results (see Appendix).

(4) In the revised version of the Cheung–Emsley paper [6 (*b*)], Emsley has adopted a value of $E_{tg}^{CC} = -0{\cdot}754\,\mathrm{kJ\,mol^{-1}}$ in the calculation of P^{iso} and results are tabulated in table 2: $P^{iso} = 0{\cdot}16$ for *ttt*, 0·41 for $tg^{\pm}t$, 0·14 for $tg^{\pm}g^{\pm}$, and 0·14 for $tg^{\pm}g^{\mp}$. The treatment is consistent within their theoretical scheme. Adoption of the value ($F_{tg}^{CC} = -3{\cdot}1\,\mathrm{kJ\,mol^{-1}}$) determined directly in the isotropic state (in acetone) [6 (*b*)], however, leads to an appreciable increase in the *gauche* fraction around the C–C bond. Combined use of $\omega = 0$ yielded $P^{iso} = 0{\cdot}10$ for *ttt*, 0·60 for $tg^{\pm}t$, 0·20 for $tg^{\pm}g^{\pm}$, and 0·0 for $tg^{\pm}g^{\mp}$ for the temperature of 342 K. These results suggest a substantial decrease of $tg^{\pm}t$ and a corresponding increase in *ttt* on going from the isotropic to the nematic state. In contrast, our model predicts that fractions of both $tg^{\pm}t$ and *ttt* should increase at the expense of the other conformers involving the *gauche* C–O form at this transition.

Although still some major discrepancies exist between the two models, the revised calculation by Emsley now predicts, in agreement with our results, that $tg^{\pm}t$ is the most stable form of DPE in both the isotropic and anisotropic states.

The authors are grateful to the Asahi Glass Foundation for financial support of this work. We wish to thank Dr S. Hiroyama of Bruker Japan Ltd. and Mr S. Tabata of Mitsubishi Chemical Co. for their technical assistance in ^{1}H NMR measurements. We would also like to thank Professor J. W. Emsley for his helpful comments on an early version of this paper.

Appendix

Conformation of DPE in the isotropic state

Conformational characteristics of DPE around the central C–C bond have been investigated in solution. The vicinal coupling constants $^3J_{HH}$ and $^3J'_{HH}$ for the $-OCH_2CH_2O-$ moiety were determined in C_6D_6 and DMSO-d_6 according to a conventional method [27]. The observed coupling constants correspond to conformational averages such as

$$^3J_{HH} = J_G f_t + \tfrac{1}{2}(J'_T + J''_G) f_g \tag{A 1}$$

$$^3J'_{HH} = J_T f_t + J'_G f_g \tag{A 2}$$

and

$$\begin{aligned} f_g &= 1 - f_t \\ &= p\sigma/(1 + p\sigma) \end{aligned} \tag{A 3}$$

where

$$p = 2\{(1 + \rho + \rho\omega)/(1 + 2\rho)\}^2 \tag{A 4}$$

Statistical weights σ and ρ are defined in figure 5. The steric interactions between the terminal phenyl and the oxygen atom separated by four bonds encountered in the $g^{\pm}g^{\mp}$ arrangement are designated by ω. As inspection of a proper model reveals, these interactions are highly repulsive in DPE, suggesting that ω may be negligibly small: $\omega \cong 0$. The RIS definition of J_Ts and J_Gs for the $-OCH_2CH_2O-$ moiety are illustrated in our previous paper [28]: for simplicity, we let $J_T = J'_T$ and $J_G = J'_G = J''_G$. Following the procedure previously described, we estimated $J_T = 11{\cdot}5$ and $J_G = 2{\cdot}25$, and $J_T = 10{\cdot}5$

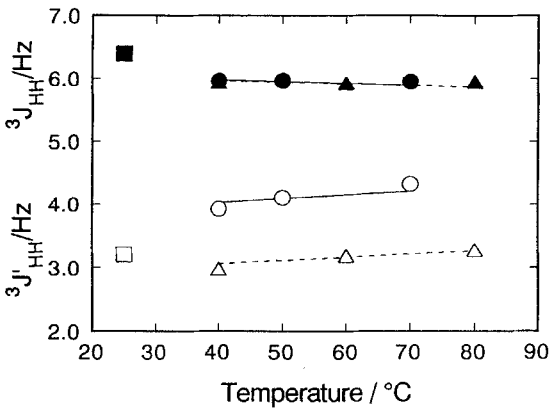

Figure A 1. Vicinal coupling constants $^3J_{HH}$ and $^3J'_{HH}$ plotted as a function of temperature: experimental values in C_6D_6 (○, ●) and in DMSO-d_6 (△, ▲). The observed trends are well reproduced by the curves calculated by using the best-fit values of J_T, J_G, and E_σ as indicated by (——) for C_6D_6 and (– –) DMSO-d_6. Also included for comparison are the corrected values of Cheung *et al.* (□, ■), measured in acetone-d_6 [6]: the temperature is arbitrarily assumed to be 25°C.

and $J_G = 2{\cdot}2$ (units being in Hz), respectively, from the measurements in C_6D_6 and DMSO-d_6. Assuming the Boltzmann relation, values of the *gauche* energy ($E\sigma$) expressed relative to the *trans* state were found to be $-2{\cdot}5$ in C_6D_6 and $-4{\cdot}4$ in DMSO-d_6, the units being kJ mol^{-1}. As shown in figure A 1, the vicinal coupling constants $^3J_{HH}$ and $^3J'_{HH}$ calculated by using these E_σ values are favourably compared with those observed over the temperature range examined. In these calculations, the conformational energy around the neighbouring C–O bond (E_ρ) was taken to be 5·5 kJ mol^{-1}, which is in the range (4·2–6·3 kJ mol^{-1}) estimated for some relevant compounds [29]. The corrected values of Cheung *et al.*'s coupling constants (in acetone-d_6 [6]) are also included in the figure. These observations lead to the conclusion that the tg$^{\pm}t$ form is somewhat more preferred in DPE in comparison with DME. More detailed analyses, including the rotational characteristics around the C–O bond, are in progress, and the results will be reported elsewhere.

References

[1] Abe, A., Iizumi, E., and Sasanuma, Y., 1993, *Polym. J.*, **25**, 1087.
[2] Gochin, M., Pines, A., Rosen, M. E., Rucker, S. P., and Schmidt, C., 1990, *Molec. Phys.*, **69**, 671. Gochin, M., Zimmermann, Z., and Pines, A., 1987, *Chem. Phys. Lett.*, **137**, 51.
[3] Photinos, J. D., Janik Poliks, B., Samulski, E. T., Terzis, A. F., and Toriumi, H., 1991, *Molec. Phys.*, **72**, 333. See also Photinos, J. D., Samulski, E. T., and Terzis, A. F., 1992, *J. phys. Chem.*, **96**, 6979.
[4] Martire, D. E., 1979, *The Molecular Physics of Liquid Crystals*, edited by G. R. Luckhurst and G. W. Gray (Academic Press), Chaps. 10, 11.
[5] Iizumi, E., 1993, Masters Dissertation, Tokyo Institute of Technology.
[6] (a) Cheung, S. T. W., and Emsley, J. W., 1993, *Liq. Crystals*, **13**, 265. (b) Emsley, J. W., 1994, *Liq. Crystals*, **16**, 671.
[7] Capinjola, J. V., 1945, *J. Am. chem. Soc.*, **67**, 1615.
[8] Zimmermann, H., 1989, *Liq. Crystals*, **4**, 591.
[9] Cope, A. C., 1935, *J. Am. chem. Soc.*, **57**, 572.
[10] Leonard, N. L., and Curry, J. W., 1952, *J. org. Chem.*, **17**, 1071.

[11] EMSLEY, J. W., LINDON, J. C., and TABONY, J. M., and WILMSHURST, T. H., 1971, *Chem. Commun.*, 1277. EMSLEY, J. W., LINDON, J. C., and TABONY, J. M., 1973, *J. chem. Soc. Faraday Trans. II*, **69,** 10. EMSLEY, J. W., LINDON, J. C., STREET, J. M., and HAWKES, G. E., 1976, *J. chem. Soc. Faraday Trans. II*, **72,** 1365.
[12] ENGLERT, V. G., and SAUPE, A., 1964, *Z. Naturf.* (*a*), **19,** 172. ENGLERT, V. G., SAUPE, A., and WEBER, J.-P., 1968, *Z. Naturf.* (*a*), **23,** 152.
[13] DIEHL, P., and KHETRAPAL, C. L., 1969, *NMR-Basic Principles and Progress*, Vol. I, edited by P. Diehl, E. Fluck and R. Kosfeld (Springer-Verlag).
[14] HSI, S., ZIMMERMANN, H., and LUZ, Z., 1978, *J. chem. Phys.*, **69,** 4126.
[15] ABE, A., and MARK, J. E., 1976, *J. Am. chem. Soc.*, **98,** 6468. SEIP, H. M., and SEIP, R., 1973, *Acta chem. Scand.*, **27,** 4024.
[16] IIJIMA, T., 1972, *Bull. chem. Soc. Japan*, **45,** 1291.
[17] ROWELL, J. C., PHILLIPS, W. D., MELBY, L. R., and PANAR, M., 1965, *J. chem. Phys.*, **43,** 3442.
[18] ELLIS, D. M., and BJORKSTAM, J. L., 1967, *J. chem. Phys.*, **46,** 4460.
[19] ABE, A., and FURUYA, H., 1988, *Molec. Crystals liq. Crystals*, **159,** 99. ABE, A., FURUYA, H., and YOON, D. Y., 1988, *Molec. Crystals liq. Crystals*, **159,** 151. ABE, A., and FURUYA, H., 1989, *Macromolecules*, **22,** 2982.
[20] SAMULSKI, E. T., 1980, *Ferroelectrics*, **30,** 83. JANIK, B., SAMULSKI, E. T., and TORIUMI, H., 1987, *J. phys. Chem.*, **91,** 1842.
[21] SASANUMA, Y., and ABE, A., 1991, *Polym. J.*, **23,** 117.
[22] WATANABE, T., NATORI, M., and OGUNI, T., 1983, *Suchikaiseki to FORTRAN*, 3rd edition (Maruzen).
[23] TASAKI, K., and ABE, A., 1985, *Polym. J.*, **17,** 641. ABE, A., TASAKI, K., and MARK, J. E., 1985, *Polym. J.*, **17,** 883. ABE, A., 1989, *Comprehensive Polymer Science*, Vol. 2, edited by C. Booth and C. Price (Pergamon), p. 49.
[24] CHEN, D. H., and LUCKHURST, G. R., 1969, *Trans. Faraday Soc.*, **65,** 656.
[25] KRONBERG, B., GILSON, D. F. R., and PATTERSON, D., 1976, *J. chem. Soc. Faraday Trans. II*, **72,** 1673, 1686.
[26] MAIER, W., and SAUPE, A., 1959, *Z. Naturf.* (*a*), **14,** 882; 1960, *Ibid.*, **15,** 287.
[27] GUTOWSKY, H. S., BELFORD, G. G., and MCMAHON, P. E., 1962, *J. chem. Phys.*, **36,** 3353.
[28] INOMATA, K., and ABE, A., 1992, *J. phys. Chem.*, **96,** 7934.
[29] ABE, A., KIMURA, N., and NAKAMURA, M., 1992, *Makromolek. Chem. Theory Simul.*, **1,** 401.